AIP | Physics of Plasmas
#1 JOURNAL IN 2014 GOOGLE SCHOLAR METRICS FOR THE PLASMA & FUSION CATEGORY

Evolution of rogue waves in dusty plasmas

R. E. Tolba, W. M. Moslem, N. A. El-Bedwehy, and S. K. El-Labany

Citation: Physics of Plasmas (1994-present) **22**, 043707 (2015); doi: 10.1063/1.4918706
View online: http://dx.doi.org/10.1063/1.4918706
View Table of Contents: http://scitation.aip.org/content/aip/journal/pop/22/4?ver=pdfcov
Published by the AIP Publishing

PHYSICS OF PLASMAS 22, 043707 (2015)

Evolution of rogue waves in dusty plasmas

R. E. Tolba,[1,a)] W. M. Moslem,[2,3,b)] N. A. El-Bedwehy,[1,c)] and S. K. El-Labany[4,d)]
[1]Department of Mathematics, Faculty of Science, Damietta University, New Damietta 34517, Egypt
[2]Department of Physics, Faculty of Science, Port Said University, Port Said 42521, Egypt
[3]Centre for Theoretical Physics, The British University in Egypt (BUE), El-Shorouk City, Cairo, Egypt
[4]Department of Physics, Faculty of Science, Damietta University, New Damietta 34517, Egypt

(Received 3 February 2015; accepted 8 April 2015; published online 24 April 2015)

The evolution of rogue waves associated with the dynamics of positively charged dust grains that interact with streaming electrons and ions is investigated. Using a perturbation method, the basic set of fluid equations is reduced to a nonlinear Schrödinger equation (NLSE). The rational solution of the NLSE is presented, which proposed as an effective tool for studying the rogue waves in Jupiter. It is found that the existence region of rogue waves depends on the dust-acoustic speed and the streaming densities of the ions and electrons. Furthermore, the supersonic rogue waves are much taller than the subsonic rogue waves by ∼25 times. © *2015 AIP Publishing LLC*.
[http://dx.doi.org/10.1063/1.4918706]

I. INTRODUCTION

A dusty plasma is a complex medium composed of massive dust particles, positive and negative ions, as well as electrons. The presence of massive dust particles can introduce new modes and instabilities in the plasma such as dust-acoustic waves and dust-ion-acoustic waves, etc.[1] On the other hand, when the mean distance between the dust particles is smaller than the Debye screening length, the charged dust grains contribute to the collective motion of the plasma. Even in the simplest case of single type of single ionized positive ions and in the absence of neutral atoms, the presence of dust grains introduces new behaviors which have been taken into account in plasma studies. It is known that the astrophysical dusty plasmas are presented in our solar system and in the interstellar environments such as in cometary tails, asteroid zones, planetary rings, interstellar medium, lower part of the earth's ionosphere, and magnetosphere (see, e.g., Refs. 2–8). Furthermore, investigations of dusty plasmas in the laboratory becomes of interest due to their importance in manufacturing processes in industry.[1] Few years ago, a simple theoretical model was presented to study the local wave phenomena taking into account the solar wind interaction with the dusty magnetospheres of planets and comets. One of the environments of dusty plasmas in our solar system is the magnetosphere of Jupiter, which was observed and examined theoretically by many authors (e.g., Refs. 9 and 10).

The nonlinear waves in dusty plasmas have been studied theoretically by many authors during the last three decades.[11–19] These investigations based on solving the nonlinear partial differential equations, which describe the plasma model, by various techniques such as perturbation methods. The obtained equations are solved either analytically or numerically to describe the physical phenomena. One of the interesting nonlinear phenomena in science (and recently in plasma physics) is the ambiguous appearance of the rogue waves. Recently, the rogue waves are investigated in a multi-component plasma and have been experimentally observed and modeled by using the nonlinear Schrödinger equation (NLSE),[20,21] while the theoretical precursors of the rogue waves in plasmas were reported by many authors (see, e.g., Refs. 22–26). Indeed, rogue waves have been studied in many different systems including nonlinear fiber optics,[27] parametrically driven capillary waves,[28] Bose-Einstein condensates,[29] superfluids,[30] optical cavities,[31] plasmonics,[32] narrow-band directional ocean waves,[33] and electromagnetic pulse propagation.[34]

In this work, it is assumed that the streaming electrons and ions of the solar wind interact with the Jupiter magnetosphere that contains positive dust grains, as well as electrons and ions. Therefore, it would be interesting to examine different plasma parameters; such as dust-acoustic speed and streaming densities, to test the existence region of the dust-acoustic rogue waves and the rogue waves profile. For this purpose, we focus our attention on the specific scenario of balancing between the group dispersion and the nonlinear effect to understand these giant waves in more details and being able to predict their occurrence.

II. THE MODEL

We consider five components unmagnetized collisionless dusty plasma composed of positive charged dust grains, streaming electrons and ions, as well as Maxwellian distribution electrons and ions. The normalized basic fluid equations of the dynamics dust grains are given by

$$\frac{\partial n_d}{\partial t} + \frac{\partial}{\partial x}(n_d u_d) = 0, \tag{1}$$

$$\frac{\partial u_d}{\partial t} + u_d \frac{\partial u_d}{\partial x} + \frac{\partial \varphi}{\partial x} = 0, \tag{2}$$

the electron beam fluid equations are

a)E-mail: tolba_math@yahoo.com.
b)E-mail: wmmoslem@hotmail.com.
c)E-mail: nab_elbedwehy@yahoo.com.
d)E-mail: skellabany@hotmail.com.

$$\frac{\partial n_c}{\partial t} + \frac{\partial}{\partial x}(n_c u_c) = 0, \tag{3}$$

$$\frac{\partial u_c}{\partial t} + u_c \frac{\partial u_c}{\partial x} + 3\mu_c\,\sigma_c \frac{\partial n_c}{\partial x} - \mu_c \frac{\partial \varphi}{\partial x} = 0, \tag{4}$$

and the ion beam fluid equations are

$$\frac{\partial n_b}{\partial t} + \frac{\partial}{\partial x}(n_b u_b) = 0, \tag{5}$$

$$\frac{\partial u_b}{\partial t} + u_b \frac{\partial u_b}{\partial x} + 3\mu_b\,\sigma_b \frac{\partial n_b}{\partial x} + \mu_b \frac{\partial \varphi}{\partial x} = 0. \tag{6}$$

The Maxwellian ions and electrons are expressed, respectively, as

$$n_i = \delta_i \exp(-s_i\,\varphi), \tag{7}$$

and

$$n_e = \delta_e \exp(s_e\,\varphi). \tag{8}$$

Equations (1)–(8) are closed by Poisson equation

$$\frac{\partial^2 \varphi}{\partial x^2} + \delta_b n_b - \delta_c n_c + \delta_i n_i - \delta_e n_e + n_d = 0, \tag{9}$$

where n_d, n_c, n_b, u_d, u_c, and u_b are the number densities of the dust grains, streaming electrons and ions, fluid velocities of the dust grains, streaming electrons and ions, respectively, φ is the electrostatic potential. The densities n_c, n_b, n_e, and n_i are normalized by $n_{d0}Z_{d0}$, n_d is normalized by n_{d0}. The space coordinate x and the time t are normalized by the Debye length $\lambda_D = (T_{eff}/4\pi n_{d0} Z_{d0} e^2)^{1/2}$ and the inverse of dusty plasma frequency $\omega_{pd}^{-1} = (m_d/4\pi n_{d0} Z_{d0}^2 e^2)^{1/2}$, while the velocities and the electrostatic potential φ are normalized by the dust-acoustic speed $C_d = (Z_{d0} T_{eff}/m_d)^{1/2}$ and T_{eff}/e, respectively. Here, $\mu_c = m_d/m_e Z_{d0}$, $\sigma_c = (T_c/T_{eff})$, $\mu_b = m_d/m_b Z_{d0}$, $\sigma_b = (T_b/T_{eff})$, $\delta_b = n_{b0}/n_{d0}Z_{d0}$, $\delta_c = n_{c0}/n_{d0}Z_{d0}$, $\delta_i = n_{i0}/n_{d0}Z_{d0}$, $\delta_e = n_{e0}/n_{d0}Z_{d0}$, $s_i = T_{eff}/T_i$, and $s_e = T_{eff}/T_e$, where $T_{e(c)}$ is the electrons (electron beam) temperature, $T_{i(b)}$ is the ion (ion beam) temperature, and $T_{eff} = Z_{d0} n_{d0} \left[\frac{n_{i0}}{T_i} + \frac{n_{e0}}{T_e}\right]^{-1}$ is the effective temperature, Z_{d0} denotes to the unperturbed dust grain charges number.

III. DERIVATION OF THE EVOLUTION EQUATION

In order to investigate the propagation of the dust-acoustic rogue waves (DARWs), we employ the reductive perturbation method.[35] According to this method, we introduce the following stretched space-time variables

$$\xi = \varepsilon^{1/2}(x - Vt) \quad \text{and} \quad \tau = \varepsilon^{3/2} t, \tag{10}$$

where ε is small parameter less than one and V is the dust-acoustic phase speed. The physical quantities appearing in Eqs. (1)–(9) $\Psi \equiv [n_d\, u_d\, n_b\, u_b\, n_c\, u_c\, n_i\, n_e\, \varphi]$ are expanded as a power series in ε about their equilibrium values as

$$\Psi = \Psi_0 + \sum_{j=1}^{\infty} \varepsilon^j \Psi_j, \tag{11}$$

where $\Psi_j = [n_{dj}\, u_{dj}\, n_{bj}\, u_{bj}\, n_{cj}\, u_{cj}\, n_{ij}\, n_{ej}\, \varphi_j]^T$ and $\Psi_0 = [1\, 0\, \delta_b\, u_{b0}\, \delta_c\, u_{c0}\, \delta_i\, \delta_e\, 0]^T$. Substituting Eqs. (10) and (11) into Eqs. (1)–(9), the lowest-order in ε gives

$$\begin{aligned} n_{d1} &= \frac{1}{V^2}\varphi_1, \quad u_{d1} = \frac{1}{V}\varphi_1, \\ n_{b1} &= \frac{\delta_b\,\mu_b}{(V-u_{b0})^2 - 3\,\delta_b^2\,\mu_b\,\sigma_b}\varphi_1, \\ u_{b1} &= \frac{(V-u_{b0})\mu_b}{(V-u_{b0})^2 - 3\delta_b^2\mu_b\sigma_b}\varphi_1, \end{aligned} \tag{12}$$

$$\begin{aligned} n_{c1} &= \frac{-\delta_c\,\mu_c}{(V-u_{c0})^2 - 3\delta_c^2\mu_c\sigma_c}\varphi_1, \\ u_{c1} &= \frac{-(V-u_{c0})\mu_c}{(V-u_{c0})^2 - 3\delta_c^2\mu_c\sigma_c}\varphi_1, \\ n_i &= -\delta_i s_i \varphi_1, \text{ and } n_e = \delta_e s_e \varphi_1. \end{aligned} \tag{13}$$

The Poisson equation gives the compatibility condition

$$\frac{1}{V^2} - s_e\delta_e^2 - s_i\delta_i^2 + \frac{\delta_b^2\,\mu_b}{(V-u_{b0})^2 - 3\delta_b^2\mu_b\sigma_b} + \frac{\delta_c^2\,\mu_c}{(V-u_{c0})^2 - 3\delta_c^2\mu_c\sigma_c} = 0. \tag{14}$$

If we consider the next-order in ε, we obtain a system of equations in the second-order perturbed quantities. Solving this system, we finally obtain the Korteweg-de Vries (KdV) equation

$$\frac{\partial \varphi_1}{\partial \tau} + A\,\varphi_1 \frac{\partial \varphi_1}{\partial \xi} + B \frac{\partial^3 \varphi_1}{\partial \xi^3} = 0, \tag{15}$$

where A and B are given by

$$A = B\left[\frac{3}{V^4} - \frac{1}{2}s_e^2\delta_e^2 + \frac{1}{2}s_i^2\delta_i^2 + \frac{3\left[(V-u_{b0})^2\delta_b^2\,\mu_b^2 + \delta_b^4\,\mu_b^3\sigma_b\right]}{\left[(V-u_{b0})^2 - 3\delta_b^2\mu_b\sigma_b\right]^3} - \frac{3\left[(V-u_{c0})^2\delta_c^2\,\mu_c^2 + \delta_c^4\,\mu_c^3\sigma_c\right]}{\left[(V-u_{c0})^2 - 3\delta_c^2\mu_c\sigma_c\right]^3}\right],$$

$$B = \frac{1}{2}\left[\frac{1}{V^3} + \frac{(V-u_{b0})\delta_b^2\,\mu_b}{\left[(V-u_{b0})^2 - 3\delta_b^2\mu_b\sigma_b\right]^2} + \frac{(V-u_{c0})\delta_c^2\,\mu_c}{\left[(V-u_{c0})^2 - 3\delta_c^2\mu_c\sigma_c\right]^2}\right]^{-1}.$$

It is well-known that the KdV equation (15) has different nonlinear solutions including solitary wave solution. However, the latter is out the scope of the present work since we are interesting to investigate the rogue waves of the evolution equation. To investigate the rogue waves, we should transfer the KdV equation to the nonlinear Schrödinger equation (NLSE). However, the NLSE that derived from the KdV equation cannot support the existence of rogue wave. We will discuss the reason in details below.

The propagation of positive and negative pulses depends on the sign of the coefficient of the nonlinear term A in the KdV Eq. (15). The pulses are positive if $A>0$ and negative when $A<0$. When the electron concentration δ_e reaches a so-called critical value (δ_{ec}), the coefficient of the nonlinear term of the KdV equation vanishes, i.e., $A=0$ for $\delta_e=\delta_{ec}$. Therefore, the KdV equation breaks down and one has to seek for another equation suitable for describing the evolution of the system at δ_{ec}. At the critical electron concentration δ_{ec}, the general method of the reductive perturbation theory introduces the modified stretched variables defined by

$$\xi=\varepsilon(x-Vt) \quad \text{and} \quad \tau=\varepsilon^3 t. \tag{16}$$

Using the stretching (16) along with the expansion (11) into the basic Eqs. (1)–(6), after some algebraic manipulations, we finally obtain the modified Korteweg-de Vries (mKdV) equation as

$$\frac{\partial\varphi_1}{\partial\tau}+C\,\varphi_1^2\frac{\partial\varphi_1}{\partial\xi}+B\frac{\partial^3\varphi_1}{\partial\xi^3}=0, \tag{17}$$

where

$$C=B\left[\frac{15}{2V^6}-\frac{1}{72}s_e^3\delta_e^2-\frac{1}{72}s_i^3\delta_i^2+\frac{15(V-u_{b0})^4\delta_b^2\mu_b^3+90(V-u_{b0})^2\delta_b^4\mu_b^4\sigma_b+27\delta_b^6\mu_b^5\sigma_b^2]}{2\left[(V-u_{b0})^2-3\delta_b^2\mu_b\sigma_b\right]^5}\right.$$
$$\left.+\frac{15(V-u_{c0})^4\delta_c^2\mu_c^3+90(V-u_{c0})^2\delta_c^4\mu_c^4\sigma_c+27\delta_c^6\mu_c^5\sigma_c^2]}{2\left[(V-u_{c0})^2-3\delta_c^2\mu_c\sigma_c\right]^5}\right].$$

Now, it is interesting to transform the mKdV Eq. (17) to the NLSE to describe the behavior of the weakly nonlinear wave-packet that gives rise to rogue wave propagation. So, we expand φ_1 (we have assumed $\varphi_1\equiv\varphi$ for simplicity hereafter) as[13]

$$\varphi(\xi,\tau)=\sum_{n=1}^{\infty}\epsilon^n\sum_{l=-n}^{n}\varphi_{l,n}(X,T)\exp il(k\,\xi-\omega\,\tau), \tag{18}$$

where k is the carrier wavenumber and ω is the frequency for the given dust-acoustic waves. The new spatial and temporal coordinates X and T are given by

$$X=\epsilon(\xi-V_g\,\tau) \quad \text{and} \quad T=\epsilon^2\tau, \tag{19}$$

where V_g is the group velocity of the envelope wavepacket to be determined later.

Assuming that all perturbed states depend on the fast scales via the phase $(k\xi-\omega\tau)$ only, while the slow scales (X, T) enter the arguments of the lth harmonic amplitude $\varphi_{l,n}$. Since $\varphi(\xi,\tau)$ must be real, the coefficients in Eq. (18) have to satisfy the condition $\varphi_{l,n}=\varphi^*_{l,n}$, where the asterisk indicates the complex conjugate. The derivative operators appearing in Eq. (17) become

$$\frac{\partial}{\partial\xi}\to\frac{\partial}{\partial\xi}+\epsilon\frac{\partial}{\partial X} \quad \text{and} \quad \frac{\partial}{\partial\tau}\to\frac{\partial}{\partial\tau}-\epsilon V_g\frac{\partial}{\partial X}+\epsilon^2\frac{\partial}{\partial T}. \tag{20}$$

Using Eqs. (18)–(20) into Eq. (17), we obtain from the first-order approximation ($n=1$) with ($l=1$) the linear dispersion relation

$$\omega=-Ck^3. \tag{21}$$

For the first harmonic of the second-order approximation ($n=2$) and ($l=1$), we calculate the group velocity as

$$V_g=-3Ck^2. \tag{22}$$

Proceeding to the third-order approximation ($n=3$) and solving for the first harmonic equations ($l=1$), an explicit compatibility condition will be found, from which we can easily obtain the nonlinear Schrödinger equation (NLSE) as

$$i\,\frac{\partial\Phi}{\partial T}+P\,\frac{\partial^2\Phi}{\partial X^2}+Q\,|\Phi|^2\Phi=0, \tag{23}$$

where $\Phi\equiv\varphi_{3,1}$. The coefficients P and Q are given by

$$P=-3Bk \quad \text{and} \quad Q=-Ck. \tag{24}$$

It is interesting to mention here that the stretched variables (16) was used instead of the stretching variables (10) since the latter cannot describe the wave propagation at $A=0$. So, we used Eq. (16) to obtain new evolution equation (17) that is valid to describe the plasma system at $A=0$. Actually, both the stretching variables (10) and (16) include the phase velocity V which is simply the dust-acoustic phase velocity. Both Eqs. (15) and (17) have spatial and temporal coordinates ξ and τ, respectively. In this frame of study, the wave can propagate with phase velocity V. When we transform equations (15) and (17) to Eq. (23) then the new wavepacket propagates with group velocity V_g. In this case, we have two different time scales the first one is for fast time scale ξ and τ with phase velocity V which is for the carrier wave. The second time scale is for the slow time scale X and T with group velocity V_g which is for the envelop wave-packet. Therefore, each of V and V_g has different physical meaning and they describe two different time scales.

IV. DISCUSSION

It is worthwhile to point out that Eqs. (15) and (17) admit soliton solution, which could be of interest if one wish to study the solitary waves of the present system. If one uses a travelling wave transformation $\eta = \xi - U\tau$, where U is the soliton speed, into Eqs. (15) and (17), the solitary wave solutions are given, respectively, by $\varphi_{1k} = \varphi_k \mathrm{sech}^2(\eta/\triangle_k)$ and $\varphi_{1m} = \varphi_m \,\mathrm{sech}(\eta/\triangle_m)$, where the subscripts k and m stand for the KdV Eq. (15) and the mKdV Eq. (17), the maximum amplitude φ_m and φ_k are given, respectively, by $3U/A$ and $\pm(6U/C)^{1/2}$, and the soliton width $\triangle_k$ and $\triangle_m$ are given, respectively, by $(4B/U)^{1/2}$ and $(B/U)^{1/2}$. Note that the soliton amplitude φ_k is proportional to the soliton speed U and is inversely proportional to the soliton width $\triangle_k$. Hence, faster solitons will be taller and narrower, while slower ones will be shorter and wider. In this work we are interesting to investigate the existence and properties of the rogue waves that may exist in the solar system, especially that in the Jupiter. Therefore, we focus our interest to examine the dependence of the existence regions on the plasma parameters those are hidden in the coefficients A, B, and C.

The character of the dynamic wave depends on the sign of the ratio of $P/Q = 3/C$. This sign refers to the (in)stability of the system. The unstable envelope pulses propagate when $P/Q > 0$, while the stable envelope pulses exist when $P/Q < 0$. On the other hand, the waves become stable if $C < 0$ and unstable if $C > 0$.

The NLSE (23) has a rational solution that is located on a nonzero background and localized both in the X and T directions[36,37] as

$$\Phi = \sqrt{\frac{P}{Q}}\left[\frac{G_0 + i\,\omega G_1}{G_2} + 1\right]\exp(i\,\omega), \tag{25}$$

where

$$\begin{aligned}
G_0 &= \frac{3}{8} - 3X^2 - 2X^4 - 9\omega^2 - 10\omega^4 - 12X^2\omega^2,\\
G_1 &= \frac{15}{4} + 6X^2 - 4X^4 - 2\omega^2 - 4\omega^4 - 8X^2\omega^2,\\
G_2 &= \frac{1}{8}\left(\frac{3}{4} + 9X^2 + 4X^4 + \frac{16}{3}X^6 + 33\omega^2 + 36\omega^4 + \frac{16}{3}\omega^6\right.\\
&\quad \left. - 24X^2\omega^2 + 16X^4\omega^2 + 16X^2\omega^4\right),\\
\omega &= QT.
\end{aligned} \tag{26}$$

Equation (25) represents the rogue wave solution within the unstable zone of the NLSE (23) for which the coefficient of the nonlinear term must be positive.

If we substitute Eqs. (18)–(20) into the KdV equation (15), we obtain also the NLSE but with different expressions of P and Q, where $P = -3Bk$ and $Q = A^2/3Bk$. Therefore, the ratio $P/Q = -1/A^2$ is always negative and hence the NLSE that obtained from the KdV equation cannot support the rogue wave solution and it is usually represent a stable wave.

Solution (25) reveals that a significant amount of the wave energy is concentrated into a relatively small area in space. This property of the nonlinear solution may serve as the basis for the explanation of the rogue wave in positive dusty plasma in Jupiter. The rogue wave is usually an envelope of a carrier wave with a wavelength smaller than the central region of the envelope. It is straightforward to see that a negative sign for P/Q is required for wave amplitude modulational stability. On the other hand, a positive sign of P/Q allows for the random perturbations grow and thus the rogue wave could be created.

Now, we discuss the rogue waves existence region and its dependence on the plasma parameters. Figures 1 and 2 show that the red region for positive P/Q and the white region stands for $P/Q < 0$. On the other hand, the rogue waves can exist within the red zone, while the dust-acoustic waves will be more structurally stable against perturbation in the white zone. It is seen that the unstable region is wide for

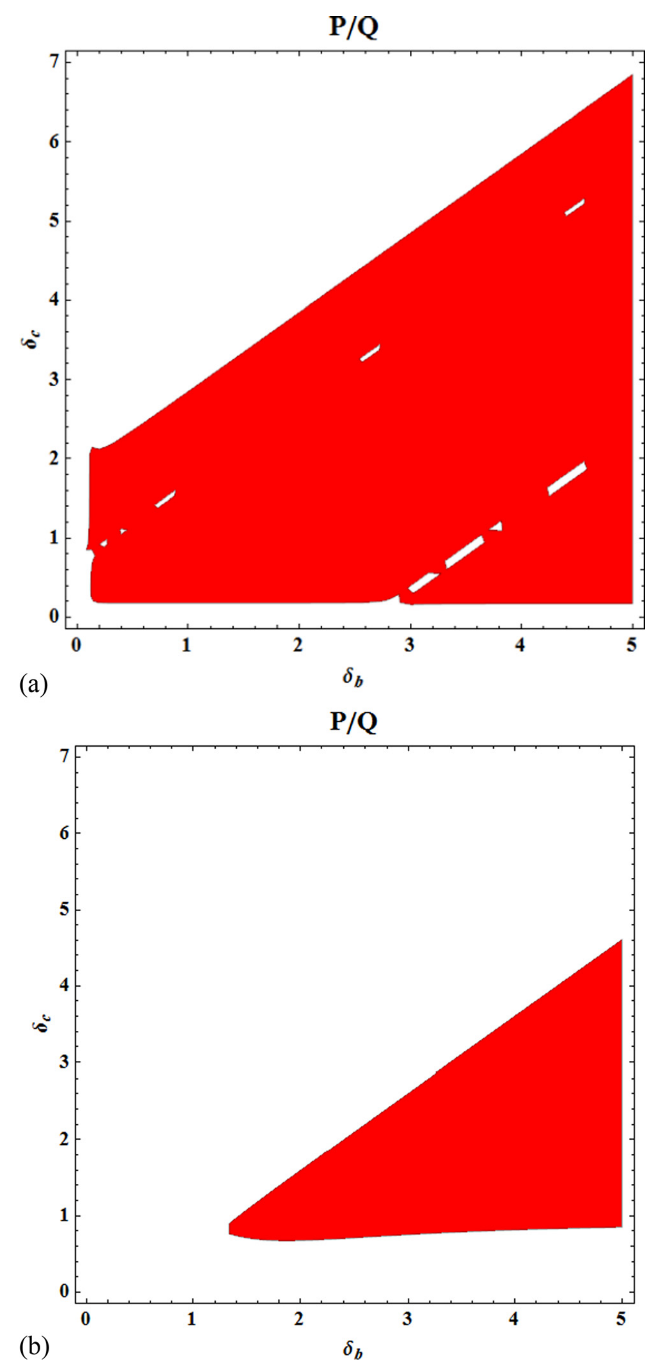

FIG. 1. The ratio P/Q contour is depicted against δ_b and δ_c for $\mu_b = 10^9$, $\mu_c = 10^{12}$, $\sigma_b = 0.5$, $\sigma_c = 0.9$, $\delta_i = 3$, $s_i = 0.9$, $u_{b0} = 8$, and $u_{c0} = 3$. (a) for $V = 0.5$ and (b) for $V = 1.5$.

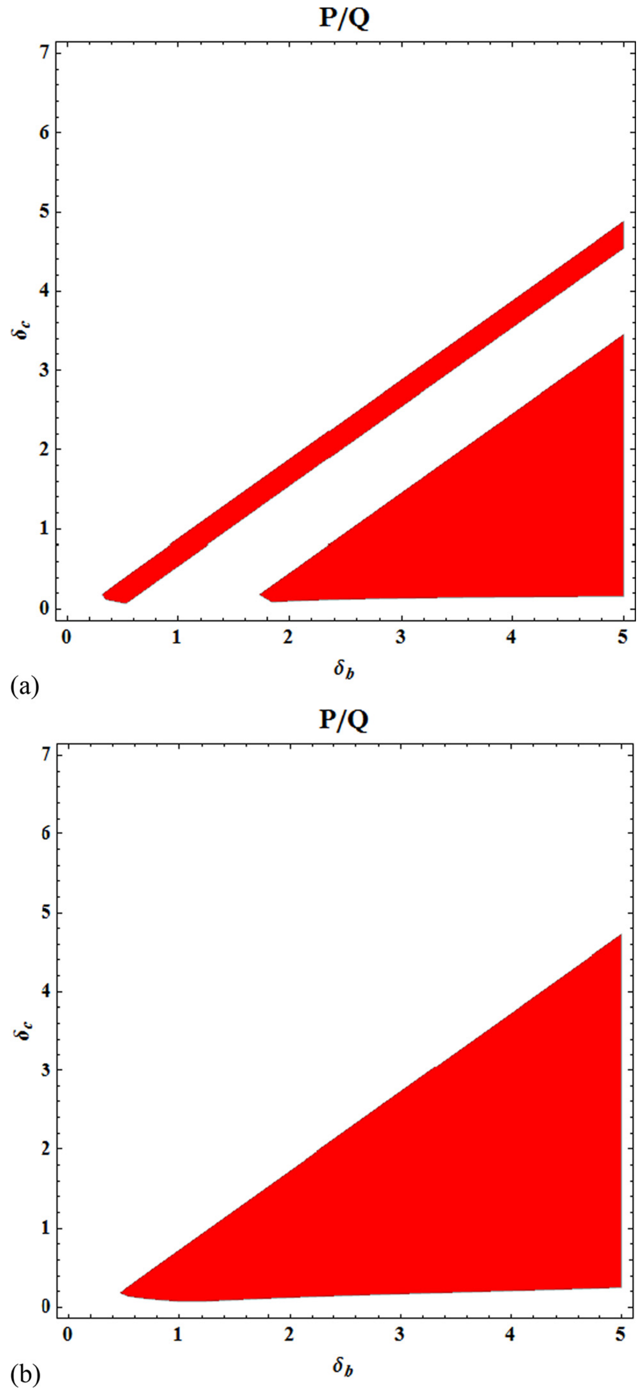

FIG. 2. The ratio P/Q contour is depicted against δ_b and δ_c for $\mu_b = 10^9$, $\mu_c = 10^{12}$, $\sigma_b = 0.5$, $\sigma_c = 0.9$, $\delta_i = 3$, $s_i = 10$, $u_{b0} = 8$, and $u_{c0} = 3$. (a) for $V = 0.5$ and (b) for $V = 1.5$.

small value of the dust-acoustic phase speed V (i.e., for subsonic pulses with $V < 1$). When the dust-acoustic phase speed V boosts to be supersonic, the instability region shrinks and the expectation region for rogue waves becomes narrower. Now, it is interesting to examine the effect of ion temperature ratio s_i as depicted in Figs. 2 and 3. Recalling that Fig. 1 is plotted for small s_i ratio (i.e., $s_i = 0.9$), however, in Figs. 2 and 3 we consider large value of s_i (i.e., $s_i = 10$). The unstable region becomes narrower with the increase of s_i for subsonic pulses (c.f. Figs. 1(a) and 2(a)). In contrast to subsonic pulses, the unstable region turns out wider for the case

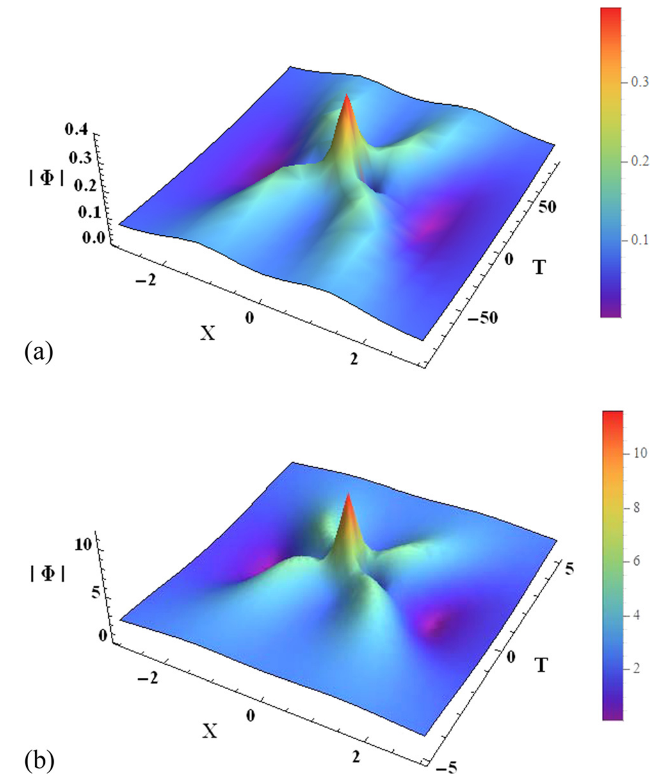

FIG. 3. The rogue waves profile for $\mu_b = 10^9$, $\mu_c = 10^{12}$, $\sigma_b = 0.5$, $\sigma_c = 0.9$, $\delta_i = 3$, $s_i = 0.9$, $u_{b0} = 8$, and $u_{c0} = 3$, (a) for $V = 0.5$, $\delta_b = 4$, $\delta_c = 1$, and (b) for $V = 1.5$, $\delta_b = 4$, $\delta_c = 3$.

of supersonic waves (c.f. Figs. 1(b) and 2(b)). Actually, this perplex relations make the investigation of rogue waves embarrassing to define the suitable regions for rogue waves

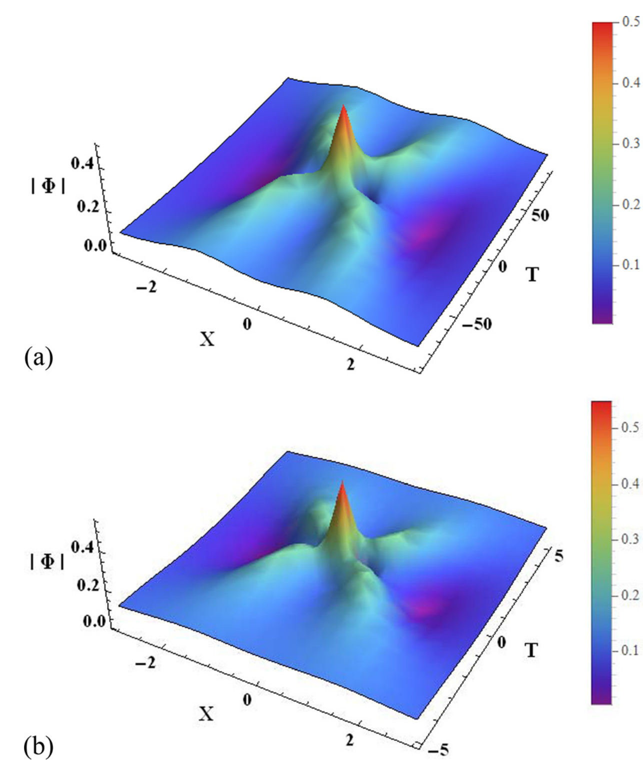

FIG. 4. The rogue waves profile for $\mu_b = 10^9$, $\mu_c = 10^{12}$, $\sigma_b = 0.5$, $\sigma_c = 0.9$, $\delta_i = 3$, $s_i = 10$, $u_{b0} = 8$, and $u_{c0} = 3$, (a) for $V = 0.5$, $\delta_b = 4$, $\delta_c = 1$, and (b) for $V = 1.5$, $\delta_b = 4$, $\delta_c = 3$.

existence. Therefore, we have to go through and investigate the other plasma parameters, which are not make a scene to change the instability regions. Indeed, Figs. 1 and 2 will be our toolbox to plot the rogue wave profile in the next figures since we have to pinpoint the parameters that give rise to rogue wave occurrence. Keeping in mind this fact, we can plot the rogue wave profile as depicted in Figs. 3 and 4. Figure 3 represents the rogue wave profile for different values of dust-acoustic phase speed ($V = 0.5$ and 1.5). It is seen that for subsonic dust-acoustic rogue waves ($V = 0.5$), the rogue wave profile has maximum amplitude $\sim$0.4. However, for supersonic dust-acoustic rogue waves ($V = 1.5$), the pulse amplitude drastically increases to be $\sim$11.5. Finally, we have considered the effect of the temperature ratio s_i on the rogue wave profile as depicted in Fig. 4. It is obvious that the increase of s_i would lead to make the subsonic pulses slightly taller (c.f. Figs. 3(a) and 4(a)). The opposite conduct happens in the case of supersonic waves and the pulses become stumpy dramatically. This behavior could be attributed to that the increase of the dust-acoustic phase speed would lead to enhance the nonlinearity and concentrate a significant amount of energy in a small region that makes the pulses taller. But when the pulses either move with subsonic speed, then the energy dissipates and drains from the system that reduces the nonlinearity and makes the pulses shorter.

V. SUMMARY

To summarize, we have investigated the behavior of the nonlinear rogue waves in five components dusty plasma composed of positive dust grains, streaming electrons and positive ions, as well as Maxwellian electrons and positive ions. It is found that at certain parameters of dust-acoustic speed, streaming densities, and temperature ratio, the perturbations could lead to the occurrence of rogue waves. The dust-acoustic phase speed, the temperature ratio, and the streaming practices number densities play a significant role in deciding how much energy could be concentrated in the rogue waves. The most important factor that makes the pulses taller is the dust-acoustic phase speed. On the other hand, the supersonic rogue waves are much taller than subsonic rogue waves by $\sim$25 times. The present results may be useful to anticipate the presence of the rogue waves in Jupiter where the positive dust grains interact nonlinearly with the streaming ions and electrons those come from the solar wind.

[1]P. K. Shukla and A. A. Mamun, *Introduction to Dusty Plasma Physics* (Institute of Physics, Bristol, 2002).
[2]M. Horanyi and D. A. Mendis, J. Astrophys. **294**, 357 (1985).
[3]P. K. Shukla, D. A. Mendis, and T. Desai, *Advances in Dusty Plasmas* (World Scientific, Singapore, 1997).
[4]C. K. Goertz, Rev. Geophys. **27**, 271, doi:10.1029/RG027i002p00271 (1989).
[5]T. G. Northrop, Phys. Scr. **45**, 475 (1992).
[6]A. Bouchule, *Dusty Plasmas* (Wiley, New York, 1999).
[7]D. Ali-Fedela, H. Marif, and M. Djebli, Adv. Space Res. **45**, 785 (2010).
[8]D. A. Mendis and M. Rosenberg, Annu. Rev. Astronomy Astrophys. **32**, 419 (1994).
[9]M. Horanyi, T. W. Hartquist, O. Havnes, D. A. Mendis, and G. E. Morfill, Rev. Geophys. **42**, RG4002, doi:10.1029/2004 RG000151 (2004).
[10]H. Saleem, Phys. Plasmas **13**, 012903 (2006); **18**, 049903 (2011); H. Saleem, W. M. Moslem, and P. K. Shukla, J. Geophy. Res. **117**, A08220 (2012).
[11]N. N. Rao, P. K. Shukla, and M. Y. Yu, Planet Space Sci. **38**, 543 (1990).
[12]P. K. Shukla and V. P. Silin, Phys. Scr. **45**, 508 (1992).
[13]S. K. El-Labany, N. A. El-Bedwehy, and H. N. Abd El-Razek, Phys. Plasmas **14**, 103704 (2007).
[14]R. Roychoudhury and S. Maitra, Phys. Plasmas **9**, 4160 (2002).
[15]Y. N. Nejoh, Aust. J. Phys. **52**, 37 (1999).
[16]S. K. El-Labany and W. F. El-Taibany, Phys. Plasmas **10**, 989 (2003); W. F. El-Taibany, A. Mushtaq, W. M. Moslem, and M. Wadati, *ibid.* **17**, 034501 (2010).
[17]W. M. Moslem, U. M. Abdelsalam, R. Sabry, and P. K. Shukla, New J. Phys. **12**, 073010 (2010); S. K. El-Labany, W. M. Moslem, N. A. El-Bedwehy, and H. N. Abd El-Razek, Astrophys. Space Sci. **337**, 231 (2012).
[18]S. K. El-Labany and W. M. Moslem, Phys. Scr. **65**, 416 (2002); S. K. El-Labany, W. M. Moslem, and M. Mahmoud, Astrophys. Space Sci. **339**, 185 (2012).
[19]M. Sadiq, S. Ali, and R. Sabry, Phys. Plasmas **16**, 013706 (2009).
[20]H. Bailung, S. K. Sharma, and Y. Nakamura, Phys. Rev. Lett. **107**, 255005 (2011).
[21]S. K. Sharma and H. Bailung, J. Geophys. Res. Space Sci. **118**, 919 (2013).
[22]L. Stenflo and M. Marklund, J. Plasma Phys. **76**, 293 (2010).
[23]W. M. Moslem, Phys. Plasmas **18**, 032301 (2011).
[24]W. M. Moslem, R. Sabry, S. K. El-Labany, and P. K. Shukla, Phys. Rev. E **84**, 066402 (2011); P. K. Shukla and W. M. Moslem, Phys. Lett. A **376**, 1125 (2012).
[25]U. M. Abdelsalam, J. Plasma Phys. **79**, 287 (2013).
[26]R. Sabry, Astrophys. Space Sci. **355**, 2141 (2014); R. Sabry, W. M. Moslem, and P. K. Shukla, Phys. Rev. E **86**, 036408 (2012).
[27]B. Kibler, J. Fatome, C. Finot, G. Millot, F. Dias, G. Genty, N. Akhmediev, and J. M. Dudley, Nature Phys. **6**, 790 (2010).
[28]M. Shats, H. Punzmann, and H. Xia, Phys. Rev. Lett. **104**, 104503 (2010).
[29]Yu. V. Bludov, V. V. Konotop, and N. Akhmediev, Phys. Rev. A **80**, 033610 (2009).
[30]A. N. Ganshin, V. B. Efimov, G. V. Kolmakov, L. P. Mezhov-Deglin, and P. V. E. McClintock, Phys. Rev. Lett. **101**, 065303 (2008).
[31]A. Montina, U. Bortolozzo, S. Residori, and F. T. Arecchi, Phys. Rev. Lett. **103**, 173901 (2009).
[32]W. M. Moslem, P. K. Shukla, and B. Eliasson, Europhys. Lett. **96**, 25002 (2011).
[33]B. Eliasson and P. K. Shukla, Phys. Rev. Lett. **105**, 014501 (2010).
[34]G. P. Veldes, J. Borhanian, M. McKerr, V. Saxena, D. J. Frantzeskakis, and I. Kourakis, J. Opt. **15**, 064003 (2013).
[35]H. Washimi and T. Taniuti, Phys. Rev. Lett. **17**, 996 (1966).
[36]S. A. El-Tantawy and W. M. Moslem, Phys. Plasmas **21**, 052112 (2014).
[37]N. Akhmediev, A. Ankiewicz, and J. M. Soto-Crespo, Phys. Rev. E **80**, 026601 (2009).